ACS Macro Letters

Letter

pubs.acs.org/macroletters



# Cluster Glasses of Semiflexible Ring Polymers

Mohammed Zakaria Slimani,[†] Petra Bacova,[‡,§] Marco Bernabei,[†,∥] Arturo Narros,[⊥] Christos N. Likos,[⊥] and Angel J. Moreno*[,†,§,#]

[†]Donostia International Physics Center, Paseo Manuel de Lardizabal 4, E-20018 San Sebastián, Spain

[‡]Departamento de Física de Materiales, Universidad del País Vasco (UPV/EHU), Apartado 1072, E-20080 San Sebastián, Spain

[§]Materials Physics Center MPC, Paseo Manuel de Lardizabal 5, E-20018 San Sebastián, Spain

[∥]Departament de Fisica Fonamental, Universitat de Barcelona, Martí i Franquès 1, E-08028 Barcelona, Spain

[⊥]Faculty of Physics, University of Vienna, Boltzmanngasse 5, A-1090 Vienna, Austria

[#]Centro de Física de Materiales (CSIC, UPV/EHU), Paseo Manuel de Lardizabal 5, E-20018 San Sebastián, Spain

Supporting Information

**ABSTRACT:** We present computer simulations of concentrated solutions of unknotted nonconcatenated semiflexible ring polymers. Unlike in their flexible counterparts, shrinking involves a strong energetic penalty, favoring interpenetration and clustering of the rings. We investigate the slow dynamics of the centers-of-mass of the rings in the amorphous cluster phase, consisting of disordered columns of oblate rings penetrated by bundles of prolate ones. Scattering functions reveal a striking decoupling of self- and collective motions. Correlations between centers-of-mass exhibit slow relaxation, as expected for an incipient glass transition, indicating the dynamic arrest of the cluster positions. However, self-correlations decay at much shorter time scales. This feature is a manifestation of the fast, continuous exchange and diffusion of the individual rings over the matrix of clusters. Our results reveal a novel scenario of glass formation in a simple monodisperse system, characterized by self-collective decoupling, soft caging, and mild dynamic heterogeneity.

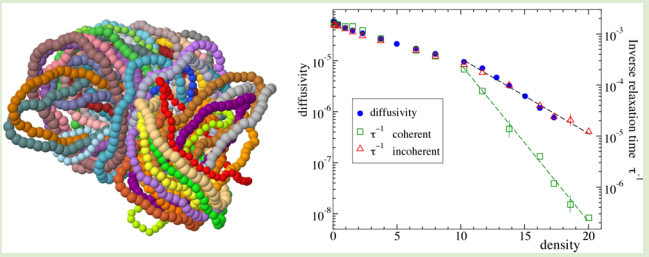


Over the last years, the fascinating properties of ring polymers have attracted the interest of researchers in the broad disciplines of physics, chemistry, biophysics, and mathematics.[1−8] The simple operation of joining permanently the two ends of a linear chain, forming a ring, has a dramatic impact on its structural and dynamic properties. This includes differences with linear chains in, e.g., their swelling,[9] rheological,[10] or scaling behavior.[11] Another remarkable effect of the ring topology is the non-Gaussian character of the effective potential in solution,[12,13] in contrast to the well-known Gaussian potential found for linear chains.[14]

The use of effective potentials reduces real macromolecular solutions to effective fluids of ultrasoft, fully penetrable particles.[14−17] This methodology facilitates the investigation of the physical properties of polymers in solution. The investigation of tunable *generic* models of ultrasoft particles, inspired by the bounded character of the real effective interactions in polymer solutions, offers a route for discovering and designing novel soft matter phases with potential realizations in real life. For a family of generic models, the so-called $Q^{\pm}$-class,[18,19] in which the Fourier transform of the bounded potential is non positive-definite, the ultrasoft particles can form clusters. At sufficiently high densities the fluid transforms into a cluster crystal.[18,19] However, the approach based on effective potentials derived *at infinite dilution* has severe limitations at high concentrations due to the emergence of many-body forces arising, e.g., from particle deformations. This has been recently demonstrated for the case of flexible ring polymers.[12]

In recent work, some of us have extended the study of ref 12 to the case of *semiflexible* rings.[20] Unlike in flexible rings, the presence of intramolecular barriers makes shrinkage energetically unfavorable. If semiflexible rings are sufficiently small, their size is only weakly perturbed.[20] This may facilitate interpenetration and promote clustering to fill the space in dense solutions. This was not the case for very small rings due to excluded-volume effects or for sufficiently long ones in which the expected random arrangement of the centers-of-mass was recovered. However, in a certain range of molecular weight an amorphous cluster phase was found, consisting of disordered columns of oblate rings penetrated by bundles of prolate rings (see Figures 12 and 13 in ref 20). This novel cluster phase emerges in a real, *one-component*, polymer solution with *purely repulsive* interactions.[20] This finding is crucially different from other soft matter cluster phases where clustering is mediated by short-range attraction and long-range repulsion.[21] Although clustering of the rings was predicted by the obtained effective

**Received:** February 25, 2014
**Accepted:** June 10, 2014
**Published:** June 12, 2014

   dx.doi.org/10.1021/mz500117v | *ACS Macro Lett.* 2014, 3, 611−616

potential, the anisotropic character of the real clusters was not captured by the *isotropic* effective interaction, which did not incorporate the relative orientation between rings as an additional, relevant degree of freedom.[20]

Recent simulations of a polydisperse (preventing crystallization) generic fluid of ultrasoft, purely repulsive particles of the $Q^{\pm}$-class have revealed the possibility of forming a *cluster glass*.[22] Whether this dynamic scenario may find a realization in a real polymer solution is an open question. Apart from the eventual inaccuracy of the ultrasoft potentials to describe real structural correlations at high concentrations (see above), predictions on the dynamics can be misleading. Even by using the correct mean-force potential describing exactly the static correlations, the real dynamics can be strongly influenced by the so-called transient forces,[23] related to the removed intramolecular degrees of freedom and not captured by the mean-force potential.

Motivated by the emergence of the anisotropic cluster state in dense solutions of semiflexible rings, in this letter we investigate the associated dynamics in this phase. We find a striking decoupling of self- and collective motions. As expected for an incipient glass transition, correlations between centers-of-mass exhibit slow relaxation, reflecting the dynamic arrest of the cluster positions. However, self-correlations relax at much shorter time scales. This feature is a manifestation of the fast, continuous exchange and diffusion of the individual rings over the quasi-static matrix of clusters. Our results reveal a novel dynamic scenario for glass formation in a real, simple monodisperse system, characterized by the simultaneous presence of self-collective decoupling, soft caging, and mild dynamic heterogeneity.

We simulate $N_R = 1600$ unknotted nonconcatenated bead−spring rings of $N = 50$ monomers. We use the monomer excluded-volume and bonding potentials of the Kremer−Grest model,[24] and implement bending stiffness.[20] We investigate the density dependence of the dynamics at fixed temperature $T = 1$ (in units of the model[20,24]). Model and simulation details are extensively described in ref 20 (here we use a friction $\gamma = 2$, instead of $\gamma = 0.5$ used in ref 20 for efficiency of equilibration). From simulations without excluded volume of the linear counterparts,[25] we have estimated a characteristic ratio[26] $C_\infty \sim 15$. This is a value typical of common stiff polymers.[26] By simple scaling, we expect to find similar trends for biopolymers ($C_\infty \sim 100$) if we use a similar ratio $N/C_\infty$. Moreover, since a bead in our model can be understood as a coarse-grained scale, our results are expected to be valid for more complex systems such as, e.g., toroidal microrings or cyclic polymer brushes, which can be currently synthesized.[27,28]

By focusing on the structure and dynamics of the centers-of-mass of the rings, we use the average diameter of gyration at infinite dilution, $D_{g0}$, to normalize the density of the ring solution. Thus, we define the density as $\rho = N_R(L/D_{g0})^{-3}$, with $L$ being the simulation box length. For $N = 50$ we find $D_{g0} = 13\sigma$, with $\sigma = 1$ as the monomer size.[20] We explored a concentration range from $\rho \to 0$ to $\rho = 20$. The value $\rho = 20$ corresponds to a monomer density of $\rho_m = 0.45$, about half the melt density in similar bead−spring models.[24]

Figure S1 in the Supporting Information shows results for the radial distribution function $g(R)$ of the centers-of-mass of the rings, at different densities. Clustering at high densities is evidenced by the increasing maximum of $g(R)$ at zero distance. Figure 1 shows results for the static structure factor of the centers-of-mass, $S(q) = N_R^{-1}\langle \sum_{j,k} \exp[i\mathbf{q}\cdot(\mathbf{R}_j(0) - \mathbf{R}_k(0))]\rangle$,

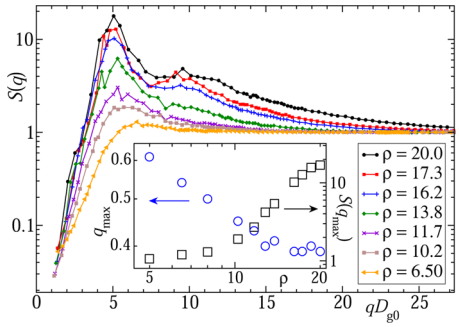


**Figure 1.** Static structure factor $S(q)$ of the centers-of-mass (main panel), for different densities (see legend). Data are represented vs the reduced wavevector $qD_{g0}$. The inset shows the density dependence of $q_{max}$ (circles) and $S(q_{max})$ (squares), where $q_{max}$ is the absolute wavevector at the maximum of $S(q)$. Both $q_{max}$ and $S(q_{max})$ are estimated by fitting the main peak to a Gaussian. The corresponding error bars are smaller than the symbol sizes in the inset.

with $\mathbf{R}_{j,k}$ denoting positions of the centers-of-mass. By increasing the concentration, $S(q)$ develops a sharp maximum at wavevector $q_{max} \sim 0.4$. This corresponds to a typical distance between centers-of-mass of $d \sim 2\pi/q_{max} \sim 16$. This is slightly higher than the typical diameter of gyration in the whole investigated density range ($12.4 < D_g < 13.6$).[20] In simple liquids the main peak is followed by a pronounced minimum $S(q_{min}) < 1$ and higher-order harmonics.[29] Instead, we find a nearly featureless, smoothly decaying shoulder extending up to large $q$-values. This reflects the full interpenetrability of the rings at short distances. The inset of Figure 1 shows the peak height $S(q_{max})$ (squares) versus the density. The slope of $S(q_{max})$ exhibits a sharp crossover at $\rho \sim 10$. We identify this feature as the onset of the cluster phase. The maximum of $S(q)$ exhibits remarkable features. Thus, it reaches values of up to $S(q_{max}) \sim 20$ at the highest investigated densities. However, these are not accompanied by crystallization, as would be expected by the Hansen−Verlet criterion for simple liquids.[30] Although the effective potential does not fully capture all details of the cluster structure (in particular its anisotropic character[20]), Figure 1 reveals a key feature of cluster-forming fluids of fully penetrable objects.[18,19] Namely, the wavevector $q_{max} \sim 0.4$ for the maximum of $S(q)$ (circles in the inset) is essentially density-independent in the cluster phase. Thus, adding rings to the system does not modify the distance between clusters ($d \sim 2\pi/q_{max}$) but just their population.[18,19]

Now we investigate the slow dynamics of the rings in the cluster phase. In standard molecular and colloidal fluids close to a glass transition,[31] particles can be mutually trapped by their neighbors over several time decades. This is the well-known caging effect, which leads to a plateau in the mean-squared displacement (MSD, $\langle \Delta r^2 \rangle$) versus time $t$. The temporal extent of the caging regime increases on approaching the glass transition (usually by increasing density and/or decreasing temperature). At longer times, particles escape from the cage and reach the diffusive regime $\langle \Delta r^2 \rangle \propto t$. Figure 2a shows the MSD of the centers-of-mass at different densities up to the highest investigated one. Data are normalized by $D_{g0}^2$ to show displacements in terms of the typical ring size. In all cases, displacements at the end of the simulation correspond to several times the ring size. Within the investigated concentration range, no plateau is found in the MSD. A soft caging effect is observed, which is manifested as an apparent subdiffusive regime $\langle \Delta r^2 \rangle \sim t^x$, with $x < 1$ decreasing by


dx.doi.org/10.1021/mz500117v | ACS Macro Lett. 2014, 3, 611−616

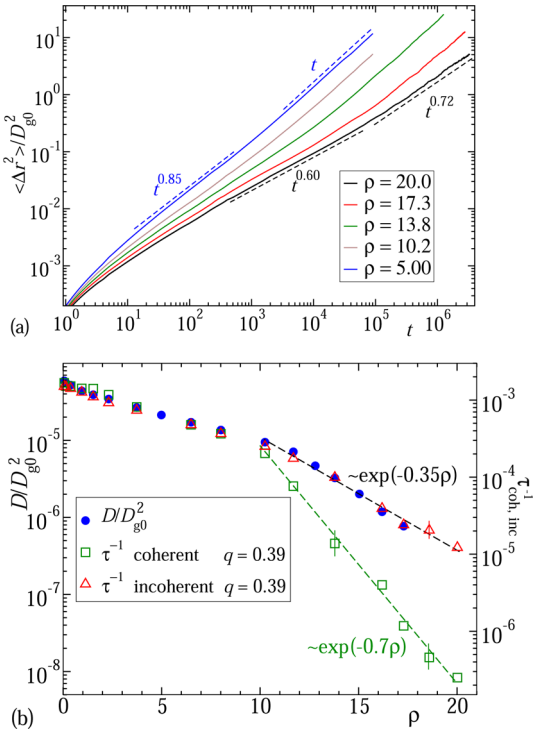


**Figure 2.** (a) MSD of the centers-of-mass (solid lines), normalized by $D_{g0}^2$, for different densities (see legend). Dashed lines describe approximate power-law behavior $\sim t^x$ (exponents given in the panel). (b) Density dependence of the diffusivity, $D$, and inverse relaxation times, $\tau^{-1}$. Some typical error bars are given. Closed circles: $D$ normalized by $D_{g0}^2$. Open symbols: $\tau^{-1}$ for the coherent (squares) and incoherent (triangles) scattering functions at $q = 0.39$. Left and right ordinate axes correspond to data of $D/D_{g0}^2$ and $\tau^{-1}$, respectively. Both ordinate axes span over the same factor $2 \times 10^4$ for a fair comparison between different data sets. The dashed lines indicate apparent exponential dependence $D$, $\tau^{-1} \sim \exp(-\Gamma\rho)$. Values of $\Gamma$ are given in the panel.

increasing concentration. The crossover to diffusive behavior is found, in most cases, when displacements approach the typical ring size, $\langle \Delta r^2 \rangle \lesssim D_{g0}^2$. However, this is not the case for the highest investigated density $\rho = 20$, where a crossover to an apparent second subdiffusive regime is found, persisting at least up to values of $\langle \Delta r^2 \rangle = 5D_{g0}^2$. The eventual crossover to diffusion is beyond the simulation time scale.

Figure 2b shows the density dependence of the diffusivity, $D$, of the centers-of-mass of the rings. This is determined as the long-time limit of $\langle \Delta r^2 \rangle / 6t$, for the densities at which the linear regime $\langle \Delta r^2 \rangle \propto t$ is reached within the simulation time scale. A sharp dynamic crossover is found at $\rho \sim 10$, i.e., around the density for the onset of the cluster phase (Figure 1). This crossover is characterized by a much stronger density dependence of the diffusivity in the cluster phase ($\rho > 10$) and, as we discuss below, a decoupling of self- and collective motions. In the investigated density range of the cluster phase, we find an apparent exponential law $D \sim \exp(-0.35\rho)$, which may suggest activated dynamics. Still, this conclusion must be taken with care because of the limited range of observation (one decade in diffusivity).

Further insight into the dynamics can be obtained by computing scattering functions of the centers-of-mass. Normalized coherent and incoherent functions are defined as $F_{coh}(q,t) = [N_R S(q)]^{-1} \langle \sum_{j,k} \exp[i\mathbf{q}\cdot(\mathbf{R}_j(t) - \mathbf{R}_k(0))] \rangle$ and $F_{inc}(q,t) = N_R^{-1} \langle \sum_j \exp[i\mathbf{q}\cdot(\mathbf{R}_j(t) - \mathbf{R}_j(0))] \rangle$, respectively. Coherent functions probe pair correlations between centers-of-mass of the rings, whereas incoherent functions probe self-correlations. Figure 3a shows results for both functions at the

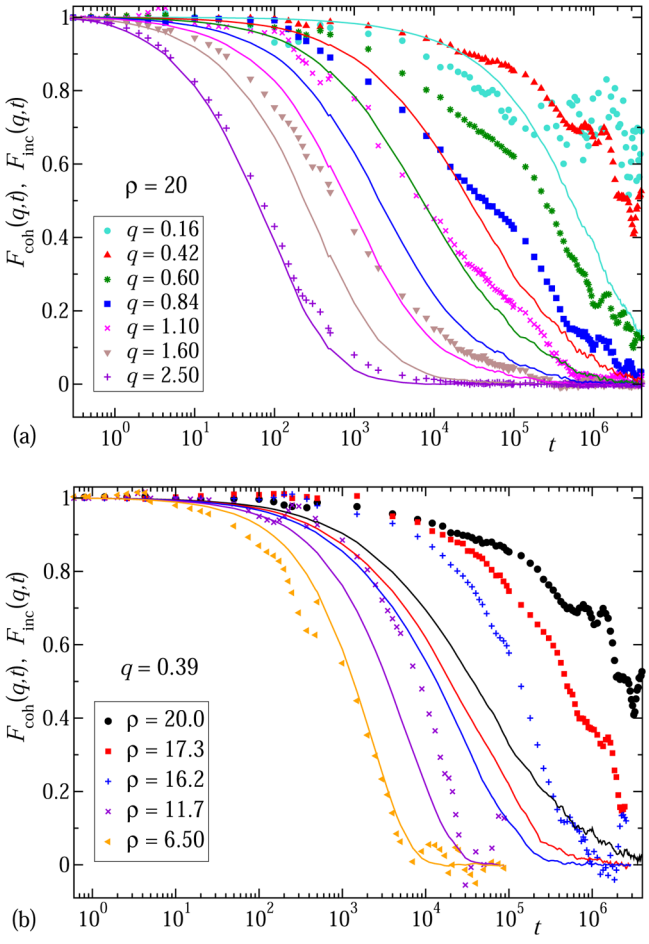


**Figure 3.** Scattering functions for the centers-of-mass of the rings. Symbols and lines correspond to coherent and incoherent functions, respectively. (a) Results for the highest investigated $\rho = 20$ and different $q$-values. (b) Results for fixed $q = 0.39 \approx q_{max}$ and different densities. In each panel, two data sets with identical colors correspond to the coherent (symbols) and incoherent (line) function for the same value of $q$ (in panel (a)) or $\rho$ (in panel (b)); see legends.

highest investigated density $\rho = 20$ and for several representative wavevectors. Comparison between data sets reveals an unusual result: the incoherent functions relax in much shorter time scales than their coherent counterparts. Only in the limit of large wavevectors $q \gg q_{max}$, where no collective correlations are really probed, both functions trivially approach each other. We illustrate this effect by representing, for $\rho = 20$, the $q$-dependence of the relaxation times $\tau$ of the scattering functions (see Figure S2 in the Supporting Information). These are defined as the times for which $F_{coh,inc}(q,\tau) = e^{-1}$. Figure 3b shows, for fixed wavevector $q = 0.39 \approx q_{max}$, coherent and incoherent scattering functions at several densities. In Figure 2b we show the density dependence of the respective inverse relaxation times, $\tau_{coh,inc}^{-1}$. As can be seen, the time scale separation between coherent and incoherent functions is associated with the onset of the cluster phase at $\rho \sim 10$ and becomes more pronounced by increasing the density. Within the whole investigated range, the incoherent inverse


dx.doi.org/10.1021/mz500117v | ACS Macro Lett. 2014, 3, 611−616

relaxation times follow the same density dependence as the diffusivity (note that both ordinate axes in Figure 2b span over the same factor $2 \times 10^4$ for a fair comparison between different data sets). In the cluster phase the inverse coherent times follow a much stronger dependence, with an apparent activation energy of about twice that of the diffusivity and incoherent inverse time.

Figure 3 demonstrates that collective correlations slow down by increasing density, reflecting the arrest of the cluster positions. This is the signature of an incipient glass transition. However, unlike in simple glass formers, this is not accompanied by a similar arrest of the self-motions, which exhibit a much faster relaxation. This reflects that fast, continuous exchange and diffusion of the rings takes place over the slowly relaxing matrix of clusters. This is consistent with the soft character of the caging regime in the MSD (Figure 2a). As discussed in ref 20, clusters are not formed in the limit of small and large rings. In Figure S3 of the Supporting Information we show results for $g(R)$ and $S(q)$ in the former two limits of noncluster forming rings (highest investigated densities for $N = 20$ and 100 in ref 20). Figure S4 of the Supporting Information shows the corresponding scattering functions. No decoupling is observed there. This further supports the intimate relation between the formation of the cluster phase and the decoupling of self- and collective motions. The small differences between coherent and incoherent functions in the noncluster forming systems can be roughly understood by simple de Gennes narrowing,[29] $\tau_{coh}/\tau_{inc} \sim S(q)$ (see Figure S5 in the Supporting Information). This is clearly not the case in the cluster phase (see Figure 4), confirming the highly nontrivial nature of the observed decoupling.

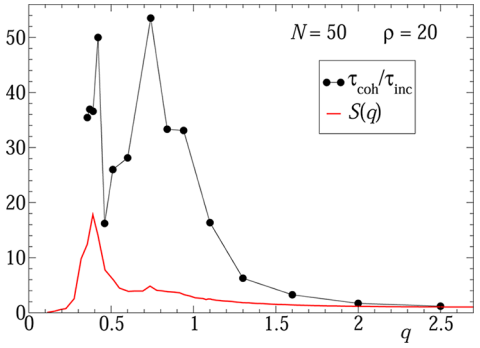


**Figure 4.** For the highest investigated density $\rho = 20$, $q$-dependence of the ratio of the coherent to the incoherent relaxation time (full black circles) and static structure factor of the centers-of-mass (thick red lines).

The dynamic scenario observed for *real* semiflexible rings, in the cluster phase, exhibits strong similarities with results in cluster glass-forming fluids of *generic* fully penetrable ultrasoft particles.[22] These include the crossover in the diffusivity to apparent activated behavior and the decoupling between coherent and incoherent dynamics in the cluster phase. Interestingly, the scenario observed for the semiflexible rings also has analogies with the dynamics in two-component systems with very strong dynamic asymmetry[32−34] and more generally in crowded environments,[35] even if clustering and penetrable ("ultrasoft") character may be absent in such systems.[32,33] Subdiffusive regimes in the MSD of the fast particles are usually observed in such mixtures, extending up to distances much larger than the particle size. The trend in Figure 2a for $\rho = 20$ resembles this feature. Decoupling of self- and collective dynamics in the mentioned mixtures is found for the fast component ("tracer"). The tracers perform large-scale fast diffusion along paths spanning over the confining matrix (formed by the slow component). Because of the slowly relaxing character of the matrix and the paths, collective correlations between the tracers decay in a much slower fashion than the self-correlations.[32−34]

The results presented here for cluster-forming semiflexible rings constitute a *novel* realization of this decoupling scenario. First, it takes place in a real *monodisperse* system. This feature is intimately connected to the fully penetrable character of the rings, which can behave both as fast "tracers" moving from one cluster to other and as part of the slow "matrix" formed by the cluster structure. Second, it is not connected to the presence of strong dynamic heterogeneities, unlike in the mentioned dynamically asymmetric mixtures[32−34] where a clear distinction between "fast" and "slow" particles exists. One might still think of a small fraction of rings performing much faster dynamics than the average, as a sort of "defect diffusion". If this were the case the van Hove self-correlation function $G_s(r,t)$ of the centers-of-mass would show, at long times, a strongly localized sharp main peak (owing to the majority slow rings), plus a secondary unlocalized peak or a broad tail corresponding to the minority fraction of fast rings. Figure 5 displays $G_s(r,t)$

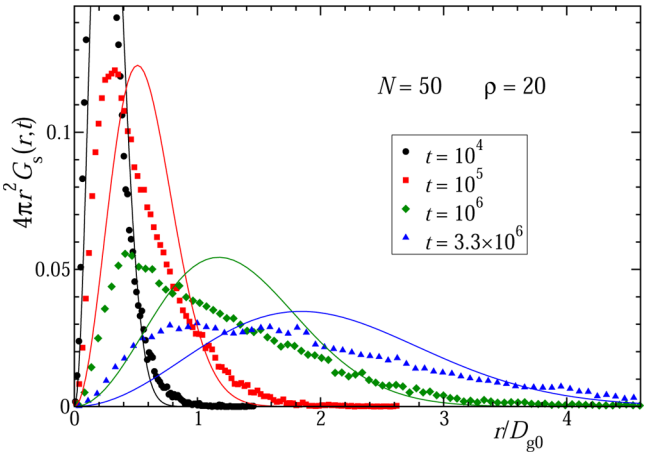


**Figure 5.** Van Hove self-correlation function of the centers-of-mass, for $N = 50$, $\rho = 20$, and at different selected times. The functions are multiplied by the phase factor $4\pi r^2$ to represent the normalized distribution of displacements. Symbols are simulation data. Lines are calculated by using Gaussian functions, $G_s(r,t) = (3/2\pi\langle r^2(t)\rangle)^{3/2} \exp[-3r^2/2\langle r^2(t)\rangle]$, with $\langle r^2(t)\rangle$ being the mean-squared displacement obtained from the simulation.

(symbols) for $\rho = 20$. This shows a smooth evolution with time. For comparison we include the results for simple Gaussian functions (lines) with the same values of $\langle \Delta r^2(t)\rangle$. Even in the most non-Gaussian case ($t = 10^6$), no putative division into two subpopulations of minority "fast" and majority "slow" rings can be made. Data in Figure 5 correspond to the usual representation of the van Hove function, which gives more weight to the fastest particles. Figure S6 in the Supporting Information shows the same data in the representation proposed in e.g., refs 36 and 37, which gives more weight to the slowest particles. Similar conclusions can be established: no putative division into subpopulations of "fast" and "slow" rings


dx.doi.org/10.1021/mz500117v | ACS Macro Lett. 2014, 3, 611−616

can be made. This is further corroborated by the fact that the diffusivity and the inverse incoherent time feature the same density dependence (Figure 2b). This is not the case in systems with strong dynamic heterogeneity, in which diffusivities and relaxation times are dominated by fast and slow particles, respectively. In conclusion, dynamic heterogeneity in the cluster phase of the rings is "mild", as opposed to the strong dynamic heterogeneity characteristic of dynamically asymmetric mixtures.[32−34]

As shown in ref 20, the cluster phase is formed by two subpopulations of rings with very different shape. The clusters consist of disordered columns of oblate rings (prolateness parameter $p \rightarrow -1$) penetrated by bundles of elongated, prolate rings ($p \rightarrow 1$). It might still be argued that the initial prolateness of the ring plays a significant role in its ulterior (fast or slow) dynamics. We find that this is not the case either. We have divided the rings into different sets according to their $p$-values at $t = 0$. Figure S7 in the Supporting Information displays the MSD, at $\rho = 20$, for several sets covering the whole $p$-range. Very weak differences are observed between the different sets. The most prolate rings are somewhat faster at early times, suggesting some enhanced longitudinal motion of the elongated bundles. However, all sets collapse for displacements smaller than the ring size. In summary, the former results indicate that all rings participate in a similar fashion, via continuous exchange between clusters, in the relaxation of the self-correlations, without any clear distinction between fast and slow subpopulations. This fast mechanism weakly alters the cluster structure, which relaxes at much longer time scales, leading to incoherent−coherent decoupling.

Although special techniques for the synthesis of pure rings have been developed,[1] the usual, high-throughput approaches inadvertently result in the presence of residual linear chains.[10] Having noted this, the qualitative picture observed here for the dynamics of the pure rings will not be affected. We performed additional simulations of a symmetric mixture of rings and linear counterparts of identical $N = 50$ (results will be presented elsewhere). Though for identical total densities less pronounced effects are observed, we anticipate that the rings in the mixture exhibit all the qualitative trends found for the pure system.

In summary, we have characterized slow dynamics in the amorphous cluster phase of a concentrated solution of unknotted nonconcatenated semiflexible rings. Our results reveal a novel dynamic scenario for glass formation in a real, simple monodisperse system, characterized by the simultaneous presence of self- and collective decoupling, soft caging, and mild dynamic heterogeneity.

## ■ ASSOCIATED CONTENT

### Supporting Information

Additional results on radial distribution functions, static structure factors, MSDs, and scattering functions, for clustering and nonclustering rings. This material is available free of charge via the Internet at http://pubs.acs.org.

## ■ AUTHOR INFORMATION

### Corresponding Author

*E-mail: wabmosea@ehu.es.

### Notes

The authors declare no competing financial interest.

## ■ ACKNOWLEDGMENTS

This work has been supported by the Austrian Science Fund (FWF), Grant No. 23400-N16. We acknowledge support from MAT2012-31088 and IT654-13 (Spain) and generous allocation of CPU time in CSUC (Spain).

## ■ REFERENCES

(1) Bielawski, C. W.; Benitez, D.; Grubbs, R. H. *Science* **2002**, *297*, 2041.
(2) Dobay, A.; Dubochet, J.; Millett, K.; Sottas, P.-E.; Stasiak, A. *Proc. Natl. Acad. Sci. U.S.A.* **2003**, *100*, 5611−5615.
(3) Moore, N. T.; Lua, R. C.; Grosberg, A. Y. *Proc. Natl. Acad. Sci. U.S.A.* **2004**, *101*, 13431−13435.
(4) Hirayama, N.; Tsurusaki, K.; Deguchi, T. *J. Phys. A: Math. Theor.* **2009**, *42*, 105001.
(5) Vettorel, T.; Grosberg, A. Y.; Kremer, K. *Phys. Biol.* **2009**, *6*, 025013.
(6) Marenduzzo, D.; Micheletti, C.; Orlandini, E. *J. Phys.: Condens. Matter* **2010**, *22*, 283102.
(7) Milner, S. T.; Newhall, J. D. *Phys. Rev. Lett.* **2010**, *105*, 208302.
(8) Micheletti, C.; Marenduzzo, D.; Orlandini, E. *Phys. Rep.* **2011**, *504*, 1−73.
(9) Jang, S. S.; Çağin, T.; Goddard, W. A., III *J. Chem. Phys.* **2003**, *119*, 1843.
(10) Kapnistos, M.; Lang, M.; Vlassopoulos, D.; Pyckhout-Hintzen, W.; Richter, D.; Cho, D.; Chang, T.; Rubinstein, M. *Nat. Mater.* **2008**, *7*, 997−1002.
(11) Halverson, J. D.; Lee, W. B.; Grest, G. S.; Grosberg, A. Y.; Kremer, K. *J. Chem. Phys.* **2011**, *134*, 204904.
(12) Narros, A.; Moreno, A. J.; Likos, C. N. *Soft Matter* **2010**, *6*, 2435−2441.
(13) Bohn, M.; Heermann, D. W. *J. Chem. Phys.* **2010**, *132*, 044904.
(14) Louis, A. A.; Bolhuis, P. G.; Hansen, J. P.; Meijer, E. J. *Phys. Rev. Lett.* **2000**, *85*, 2522−2525.
(15) Likos, C. N. *Phys. Rep.* **2001**, *348*, 267−439.
(16) Gottwald, D.; Likos, C. N.; Kahl, G.; Löwen, H. *Phys. Rev. Lett.* **2004**, *92*, 068301.
(17) Mladek, B. M.; Kahl, G.; Likos, C. N. *Phys. Rev. Lett.* **2008**, *100*, 028301.
(18) Likos, C. N.; Mladek, B. M.; Gottwald, D.; Kahl, G. *J. Chem. Phys.* **2007**, *126*, 224502.
(19) Mladek, B. M.; Gottwald, D.; Kahl, G.; Neumann, M.; Likos, C. N. *Phys. Rev. Lett.* **2006**, *96*, 045701.
(20) Bernabei, M.; Bacova, P.; Moreno, A. J.; Narros, A.; Likos, C. N. *Soft Matter* **2013**, *9*, 1287−1300.
(21) Cardinaux, F.; Zaccarelli, E.; Stradner, A.; Bucciarelli, S.; Farago, B.; Egelhaaf, S. U.; Sciortino, F.; Schurtenberger, P. *J. Phys. Chem. B* **2011**, *115*, 7227−7237.
(22) Coslovich, D.; Bernabei, M.; Moreno, A. J. *J. Chem. Phys.* **2012**, *137*, 184904.
(23) Briels, W. J. *Soft Matter* **2009**, *5*, 4401.
(24) Kremer, K.; Grest, G. S. *J. Chem. Phys.* **1990**, *92*, 5057−5086.
(25) We simulate isolated linear chains by keeping the bonding and bending potentials. To keep the bond length and to obtain long-range Gaussian statistics, monomer excluded volume is switched off except for mutually connected monomers. $C_\infty$ is obtained by analyzing the scaling behavior of the intramolecular distances.[26]
(26) Rubinstein, M.; Colby, R. H. *Polymer Physics*; Oxford University Press, Inc.: New York, 2003.
(27) Lee, J.; Baek, K.; Kim, M.; Yun, G.; Ko, Y. H.; Lee, N. S.; Hwang, I.; Kim, J.; Natarajan, R.; Park, C. G.; Sung, W.; Kim, K. *Nat. Chem.* **2014**, *6*, 97−103.
(28) Zhang, K.; Zha, Y.; Peng, B.; Chen, Y.; Tew, G. N. *J. Am. Chem. Soc.* **2013**, *135*, 15994−15997.
(29) Hansen, J.-P.; McDonald, I. *Theory of Simple Liquids*, 3rd ed.; Academic Press: New York, 2006.
(30) Hansen, J. P.; Verlet, L. *Phys. Rev.* **1969**, *184*, 151.

(31) Binder, K.; Kob, W. *Glassy Materials and Disordered Solids*; World Scientific: River Edge, NJ, 2005.
(32) Horbach, J.; Kob, W.; Binder, K. *Phys. Rev. Lett.* **2002**, *88*, 125502.
(33) Moreno, A. J.; Colmenero, J. *J. Chem. Phys.* **2006**, *125*, 164507.
(34) Mayer, C.; Sciortino, F.; Likos, C. N.; Tartaglia, P.; Löwen, H.; Zaccarelli, E. *Macromolecules* **2009**, *42*, 423.
(35) Coslovich, D.; Kahl, G.; Krakoviack, V. *J. Phys.: Condens. Matter* **2011**, *23*, 230302.
(36) Puertas, A. M.; Fuchs, M.; Cates, M. E. *J. Chem. Phys.* **2004**, *121*, 2813−2822.
(37) Szamel, G.; Flenner, E. *Phys. Rev. E* **2006**, *73*, 011504.